Journal of Statistical Physics, Vol. 85, Nos. 3/4, 1996

Two-Dimensional Oriented Self-Avoiding Walks with Parallel Contacts

G. T. Barkema[1] and S. Flesia[2,3]

Received December 18, 1995; final March 28, 1996

Oriented self-avoiding walks (OSAWs) on a square lattice are studied, with binding energies between steps that are oriented parallel across a face of the lattice. By means of exact enumeration and Monte Carlo simulation, we reconstruct the shape of the partition function and show that this system features a first-order phase transition from a free phase to a tight-spiral phase at $\beta_c = \log(\mu)$, where $\mu = 2.638$ is the growth constant for SAWs. With Monte Carlo simulations we show that parallel contacts happen predominantly between a step close to the end of the OSAW and another step nearby; this appears to cause the expected number of parallel contacts to saturate at large lengths of the OSAW.

KEY WORDS: Self-avoiding walks; oriented walks; collapse; spiral walks; Monte Carlo; exact enumeration.

1. INTRODUCTION

Many aspects of the behavior of polymers can be described by self-avoiding walks on a lattice. Some polymers have interactions that depend on the spatial orientation of the polymer, for instance A–B polyester. Such polymers are conveniently modeled by oriented self-avoiding walks (OSAW) with two types of short-ranged interaction between edges, depending on their relative orientation.[1–4]

The model of investigation in this paper consists of one OSAW on a square lattice. Besides self-avoidance, the only interactions of the OSAW with itself occur if two steps of the walk are one lattice spacing apart. If the

[1] Institute for Advanced Study, Princeton, New Jersey 08540.
[2] Theoretical Physics, University of Oxford, Oxford, OX1 3NP, United Kingdom.
[3] Present address: Department of Mathematics, Imperial College, London SW7 2BZ, United Kingdom.

822/85/3-4-5*

two steps have the same orientation, they are said to form a *parallel contact*, to which an energy gain of ε_p is attributed. If they have opposite orientation, they are said to form an *antiparallel contact*, with an energy gain of ε_a. If β is the inverse temperature and we define $\beta_p = -\beta\varepsilon_p$ and $\beta_a = -\beta\varepsilon_a$ then the partition function of such an oriented self-avoiding walk is given by

$$Z_n(\beta_p, \beta_a) = \sum_{m_p, m_a} C_n(m_p, m_a)\, e^{\beta_p m_p + \beta_a m_a} \tag{1}$$

where the sum is over all allowed values of the number of parallel contacts m_p and the number of antiparallel contacts m_a and $C_n(m_p, m_a)$ is the number of configurations of length n with m_p parallel and m_a antiparallel contacts. The limiting reduced free energy per step is given by

$$F(\beta_p, \beta_a) = \lim_{n \to \infty} \frac{1}{n} \log[Z_n(\beta_p, \beta_a)] \tag{2}$$

The phase diagram of this model was studied previously[2]; numerical results from exact series up to $n = 29$ edges showed the existence of three phases: a free SAW phase, a normal collapsed phase; and a compact spiral phase. The transition from the free to the spiral phase was conjectured to be of first order.

In this article we will concentrate on the case where there are only interactions between parallel contacts, i.e., $\beta_a = 0$. The earlier work[2] rigorously proved that for this case the reduced limiting free energy is constant for $\beta_p \leqslant 0$ with value $\log(\mu)$, where μ is the growth constant for the SAW ($\mu = 2.638$). For $\beta_p > 0$ the following rigorous bounds were proved:

$$\beta_p \leqslant F(\beta_p, 0) \leqslant \beta_p + \log(\mu) \tag{3}$$

The above results prove the existence of a phase transition for $0 \leqslant \beta_p \leqslant \log(\mu)$. Bennett-Wood *et al.*[2] conjectured that the critical inverse temperature β_c is near or equal to the lower bound which, for $\beta_a = 0$, is $\log(\mu) \approx 1$. In section 2 we further investigate this phase transition by extending the exact enumeration data, by means of Monte Carlo results and combining them with some rigorous results on tight spirals.

Another interesting question concerning OSAWs is the mean number of contacts. Flesia[3] proved that for the mean number of antiparallel contacts one has $\langle m_a \rangle \sim n$ in two or higher dimensions, where n is the number of steps of the walk. The mean number of parallel contacts scales as $\langle m_p \rangle \sim n$ in three or higher dimensions, but in two dimensions the behavior is still an open question. Field-theoretic work[1] predicts that in

two dimensions $\langle m_p \rangle \sim \log(n)$ in the limit $n \to \infty$. However, Monte Carlo results for OSAWs with up to 3000 steps seem to indicate that $\langle m_p \rangle$ tends to a constant ~ 0.05.[3] In section 3 we present the results of large-scale Monte Carlo simulations with OSAWs of up to 5000 steps, and investigate these results in a way that allows extrapolations to even larger n. Based on these results we obtain an upper bound for $\langle m_p \rangle$ in the limit $n \to \infty$.

2. PHASE TRANSITION TOWARD A TIGHT SPIRAL

Bennett-Wood *et al.*[2] enumerated all configurations up to SAWs with a length of $n = 29$ and ordered them according to their number of parallel and antiparallel contacts. We extended the exact enumeration of the OSAWs with parallel contacts, and obtained all values for $C_n(m_p)$, the number of OSAWs consisting of n steps and having m_p parallel contacts, up to $n = 34$.

In our enumeration program, we start with generating all OSAWs of length $l \leqslant n$ with a parallel contact between the first and the last step. For each walk w, we determine the number of parallel contacts m_w. We also

Table I. Exact Enumeration of the Number of OSAWs of n Steps with m_p Parallel Contacts

n	$m_p = 0$	1	2	3	4	
30	4173469695963	61649050972	8921988104	1417268612	221155744	
31	10975225680123	163203273852	25422408744	3820038428	663920466	
32	29224474453695	453395153136	67676366244	11044497696	1800473376	
33	77923458322683	1201209580824	190907785004	29775283928	5291859172	
34	207390873801535	3318007864896	508582438722	84979159776	14355126160	
	5	6	7	8	9	
30	35795108	5383888	801432	108062	16652	
31	98665196	17463042	2253640	399888	46368	
32	301423940	48238616	7546064	1123840	177756	
33	830969056	150009218	21332880	3819684	510908	
34	2474324280	415293124	67773784	10824900	1773072	
	10	11	12	13	14	15
30	1372	272	16			
31	7188	640	164			
32	20000	3512	332	48		
33	81240	10096	1976	72	28	
34	235146	40728	5294	704	40	16

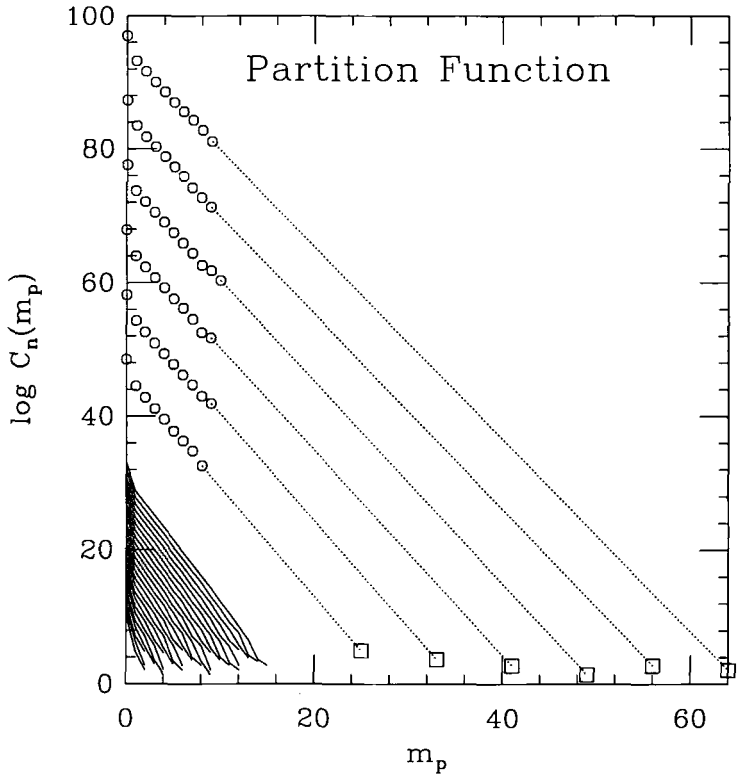

Fig. 1. A graphical representation of the partition function: the logarithm of the number of OSAWs is plotted as a function of its number of parallel contacts. Solid lines are data for $n = 11 \cdots 34$, obtained from exact enumeration, circles are data for $n = 50$, 60, 70, 80, 90, and 100, obtained from Monte Carlo simulations, squares are from properties of tight spirals, and the dotted lines connect the Monte Carlo results with the corresponding results for tight spirals.

determine $M_i(w, t_i, m_i)$, the number of extensions on the inside end of walk w with length $t_i \leqslant n - l$ and m_i parallel contacts with either itself or w, and $M_o(w, t_o, m_o)$, the corresponding quantity for the extensions on the outside end. Since the walk w prevents contacts between the inside and outside extensions, the total number of OSAWs of length n with m_p parallel contacts is given by

$$Z_n(m_p) = \frac{1}{m_p} \sum_{w} \sum_{l + t_i + t_o = n} M_i(w, t_i, m_i)\, M_o(w, t_o, m_o)\, \delta(m_p, m_w + m_i + m_o) \tag{4}$$

The prefactor in this equation corrects for the fact that there are m_p different walks w from which we can generate the same OSAW with m_p parallel contacts. Exploiting rotational and mirror symmetry, we enumerated all OSAWs of length $n \leqslant 34$ with one or more parallel contacts in a run of about 2 weeks on a four-processor DEC alpha workstation. Finally, the number of OSAWs without parallel contacts is obtained by subtraction from the total number of OSAWs (from ref. 7).

The results are given in Table I, and plotted as the solid lines in Fig. 1, where $\log[C_n(m_p)]$ is plotted as a function of m_p. The figure shows that up to $n = 34$, the number of configurations as a function of the number of parallel contacts first drops quickly with a factor p_n, but then, over the whole range $1 \leqslant m_p \leqslant m_{\max}$ falls off exponentially with the same exponent q_n. The partition function $Z_n(\beta_p)$ is thus described well by

$$\begin{aligned} C_n(1) &= p_n C_n(0) \\ C_n(m) &\approx C_n(1) \exp[-q_n(m-1)] \end{aligned} \tag{5}$$

where p_n and q_n are n-dependent parameters.

To extend the graph presenting the partition function beyond $n = 34$ by means of exact enumeration is very hard. However, the left part of this graph for much larger n can be obtained statistically by means of Monte Carlo simulations: OSAWs are randomly generated with the pivot algorithm[5] and a histogram is made of the number of parallel contacts of these OSAWs. This gives us a direct measurement of $C_n(m_p)/Z_n(0)$ for a small number of parallel contacts. In our Monte Carlo simulations, we thermalized over 10^7 pivot moves, followed by 10^8 moves to gather statistics; statistical errors were obtained by repeating the whole procedure ten times. The results are shown in Table II; the density of OSAWs with more than ~ 10 parallel contacts is so small that they will most likely never be generated, and we only obtain an upper bound for them. A good approximation for $Z_n(0)$ is known:

$$Z_n(0) \approx (A/4)\, \mu^n n^{\gamma_s - 1} \tag{6}$$

where $\mu = 2.638$, $\gamma_s = 43/32$,[6] and $A = 1.771$.[7] The factor of one fourth is due to the fact that we count OSAWs that are equivalent after rotation only once. The Monte Carlo results from Table II for $n = 50$, 60, 70, 80, 90, and 100, multiplied by $Z_n(0)$, are plotted as circles in the left side of Fig. 1.

Also the rightmost point of the graph can be obtained, as there the only relevant configurations are tight spirals. The corners of a tight spiral are reached after $n = k, k+1, 2k+2, 2k+4, 3k+6, 3k+9,...$ steps, i.e., at $n = ik + i^2$ or $n = ik + i(i-1)$, where k is the number of steps in the same

Table II. Monte Carlo Results for the Density of OSAWs of Length n with m_p Parallel Contacts

n	$m_p=0$	1	2	3	4
50	0.97763(1)	0.01841(1)	0.003209(8)	0.000599(3)	0.000120(1)
60	0.97603(2)	0.01954(2)	0.003555(7)	0.000696(3)	0.0001426(8)
70	0.97479(3)	0.02039(3)	0.003832(7)	0.000780(4)	0.000164(1)
80	0.97368(2)	0.02118(2)	0.004067(10)	0.000840(6)	0.000180(2)
90	0.97280(3)	0.02178(2)	0.00426(1)	0.000903(3)	0.000198(2)
100	0.97210(2)	0.02229(2)	0.00441(1)	0.000933(4)	0.000209(2)
1000	0.9629(4)	0.0284(3)	0.0066(1)	0.00159(7)	0.00042(2)
2000	0.9618(4)	0.0293(5)	0.0067(1)	0.00166(5)	0.00043(4)
	5	6	7	8	9
50	0.0000233(4)	0.0000052(3)	0.00000112(9)	0.00000012(3)	0.00000002(2)
60	0.0000300(5)	0.0000062(2)	0.0000013(1)	0.00000026(5)	0.00000008(2)
70	0.0000346(6)	0.0000080(3)	0.0000015(2)	0.00000021(4)	0.00000009(4)
80	0.0000401(8)	0.0000087(5)	0.0000019(2)	0.00000032(7)	0.00000014(3)
90	0.000044(1)	0.0000109(3)	0.0000020(2)	0.00000045(6)	0.00000011(4)
100	0.000047(1)	0.0000112(5)	0.0000029(2)	0.0000007(1)	0.00000012(4)
1000	0.000102(8)	0.000032(6)	0.000009(2)	0.0000007(4)	
2000	0.00012(2)	0.000024(5)	0.000009(3)	0.0000010(4)	

direction at the inner end of the tight spiral, and i is a positive integer. Each additional step of the tight spiral adds one parallel contact, except steps before and after a corner. Thus, the number of parallel contacts $m_{\max}$ for an OSAW of length n is given by

$$\text{if } n \leqslant 2k: \quad m_{\max} = 0$$

$$\text{if } n > 2k: \quad m_{\max} = n - 2k + 3 - \left[\left(n + \frac{k^2}{4}\right)^{1/2} - \frac{k}{2}\right] - \left[\left(n + \frac{k^2}{4} - 1\right)^{1/2} - \frac{k}{2}\right] - \left[\left(n + \frac{(k-1)^2}{4}\right)^{1/2} - \frac{k-1}{2}\right] - \left[\left(n + \frac{(k-1)^2}{4} - 1\right)^{1/2} - \frac{k-1}{2}\right] \tag{7}$$

where square brackets denote the Entier function ($[x]$ is the largest integer not larger than x). The number of parallel contacts of a "rectangular" tight spiral (with $k > 1$) never exceeds that of the "square" tight spiral (with $k = 1$), but they can be equal, adding to the degeneracy of the ground state. Additional ground states can be generated by removing steps from the inside and adding them to the outside end, until the corner is reached.

Also, if the tight spiral ends at a corner or one or two steps further, additional ground states arise by rearranging these last steps.

We enumerated all OSAWs with $m_{\max}$ parallel contacts and length up to $n = 50$, and confirmed that all ground states can be generated with these operations. Assuming that no new types of degenerate ground states arise after $n = 50$, we calculated the degeneracy of the ground state for lengths up to one million steps, and observed that the degeneracy fluctuates between 4 (for a complete "square" tight spiral) and $c_m n^{3/4}$ with $c_m = 5.3$, whereas the expected degeneracy grows as $c_a n^{3/4}$ with $c_a = 2.1$. For $n = 50$, 60, 70, 80, 90 and 100, there are 140, 40, 16, 4, 16, and 8 configurations with the maximum number of parallel contacts. We have added these results of the tight spirals in Fig. 1 as squares.

For $n \gg 34$, the Monte Carlo data in Fig. 1 for small m_p do not extrapolate to the exact results for tight spirals, but point below, which suggest that Eq. (5) is an upper bound for $n \gg 34$. The dotted lines in Fig. 1 represent these upper bounds. We cannot exclude the possibility that for $n \gg 34$ the partition function initially stays below these dotted lines, then increases and crosses this dotted line for intermediate values of m_p, and finally reaches the exact result for tight spirals; however, we think that that scenario is unlikely, and the results concerning long OSAWs in the remainder of this section are based on the assumption that the dotted lines in Fig. 1 represent upper bounds.

For $n \leqslant 34$ we know $C_n(0)$ and $C_n(1)$ by exact enumeration, and for $n = 50$, 60, 70, 80, 90, 100, 1000, and 2000 we know $C_n(0)/Z_n$ and $C_n(1)/Z_n$ accurately from the Monte Carlo simulations. This enables us to compute p_n in Eq. (5) for all these values of n. For large n, p_n converges to a constant value around 0.031. To extract the specific heat and density of parallel contacts, we used a fit to p_n which is given by

$$p_n - p_\infty \sim (1/\sqrt{n}) \tag{8}$$

where $p_\infty = 0.031 \pm 0.002$. We can obtain the values q_n in Eq. 5 from (6)–(8) as

$$q_n \approx \frac{\log(C_n(1)) - \log(C_n(m_{\max}))}{m_{\max} - 1} \approx \frac{\log(Z_n) + \log(p_n) - \frac{3}{4}\log(n)}{m_{\max} - 1} \tag{9}$$

For $n = 1000$ and 2000, this equation predicts that $q_n = 1.099$ and 1.060, respectively, whereas the Monte Carlo results in table II for $C_n(1)/C_n(5)$ indicate that the slope of $\log(C_n(m_p))$ corresponds to values of $q_n \approx 1.4$; for larger values of n the curves of $\log(C_n(m_p))$ versus m_p initially point below the point corresponding to the tight-spiral configuration, and thus must bend upward at larger m_p.

For n up to 34 we plot in Fig. 2 the specific heat, defined by $\beta_\chi = -\partial^2 F/\partial\beta^2$, and in Fig. 3 we plot the density of parallel contacts $\langle m_p \rangle / n$, as a function of the inverse temperature β. In both figures we add the graphs for $n = 50$, 100, 200, 500, 1000, 2000 and 10,000, obtained from Eq. (5), as dotted lines. In Fig. 2, the value of β where the peak of the specific heat is located is moving backward to $\beta = \log(\mu)$, as is the point where $\langle m_p \rangle / n$ is increasing steeply in Fig. 3. The jump in the density of parallel contacts (i.e., the energy density) is increasing with increasing n, indicating a first order transition. In fact, assuming Eq. (5) one can show analytically that in the limit $n \to \infty$ the function $\langle m_p \rangle / n$ approaches the Heaviside step function $\Theta(\log(\mu))$, and this still holds if Eq. (5) is an upper bound rather than an exact expression in the regime between tight spirals and walks with few parallel contacts. Both the specific heat and the density of parallel contacts are insensitive to the fact mentioned earlier, that the curve starts somewhat steeper at small m_p and thus must bend up at larger m_p. If anything, this will increase the peak value of the specific heat, and the steepness of the density curve.

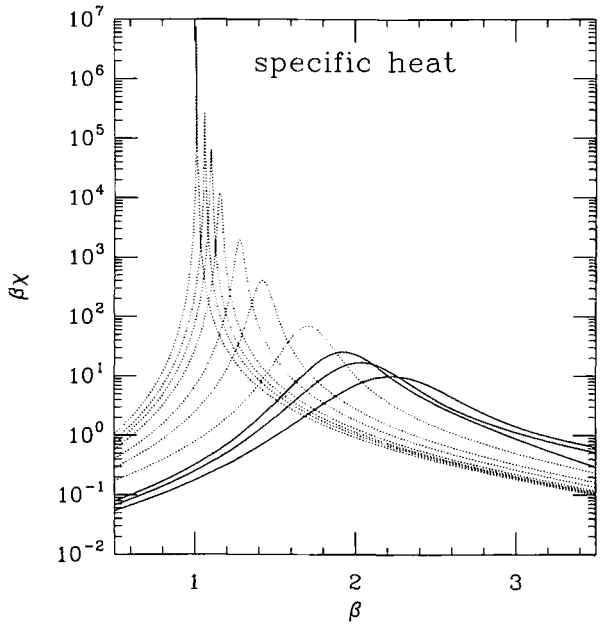

Fig. 2. Specific heat as a function of inverse temperature β. In the direction of increasing peak value, the curves are obtained for $n = 25$, 30, and 34 from exact enumeration (solid lines) and for $n = 50$, 100, 200, 500, 1000, 2000, and 10,000 from Eq. (4) (dotted lines).

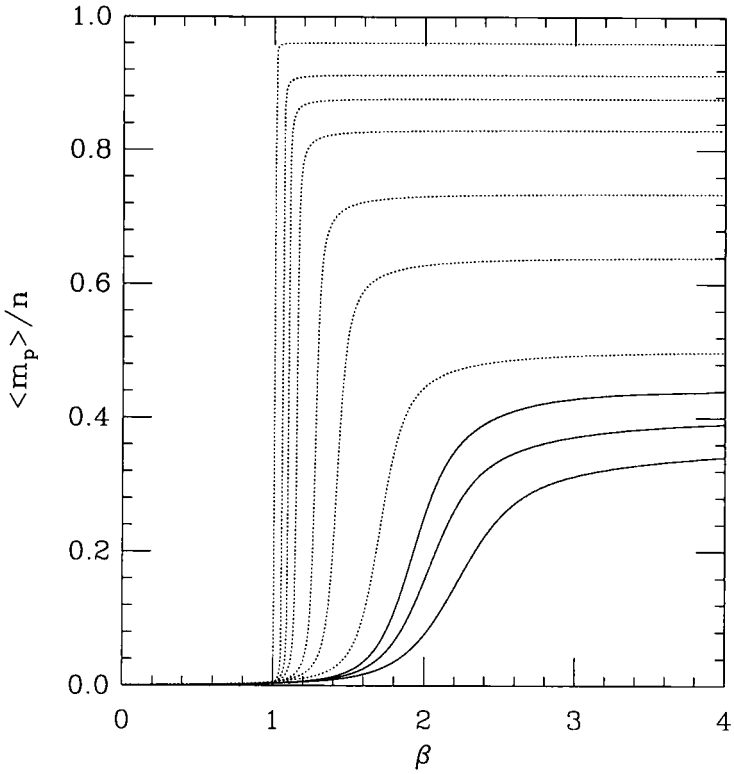

Fig. 3. Density of parallel contacts as a function of inverse temperature β. In the direction of increasing density, the curves are obtained for $n = 25$, 30, and 34 from exact enumeration (solid lines) and for $n = 50$, 100, 200, 500, 1000, 2000, and 10,000 from Eq. (4) (dotted lines).

Another way to estimate the transition point is to look at the zeroes of the partition function.[8, 9] The partition function of an OSAW of n steps with m_p parallel contacts is a polynomial of degree $m_{\max}$ (the maximum number of parallel contacts) in the variable $x = e^{\beta}$, hence it can be conveniently written in terms of its n roots r_{m_p} in the complex plane:

$$Z_n(x) = C_n(0) \prod_{m_p=1}^{m_{\max}} 1 - (x/r_{m_p}) \tag{10}$$

and the free energy per steps

$$F_n(x) = \frac{1}{n} \log(C_n(0)) + \frac{1}{n} \sum_{m_p=1}^{m_{\max}} \log\left(1 - \frac{x}{r_{m_p}}\right) \tag{11}$$

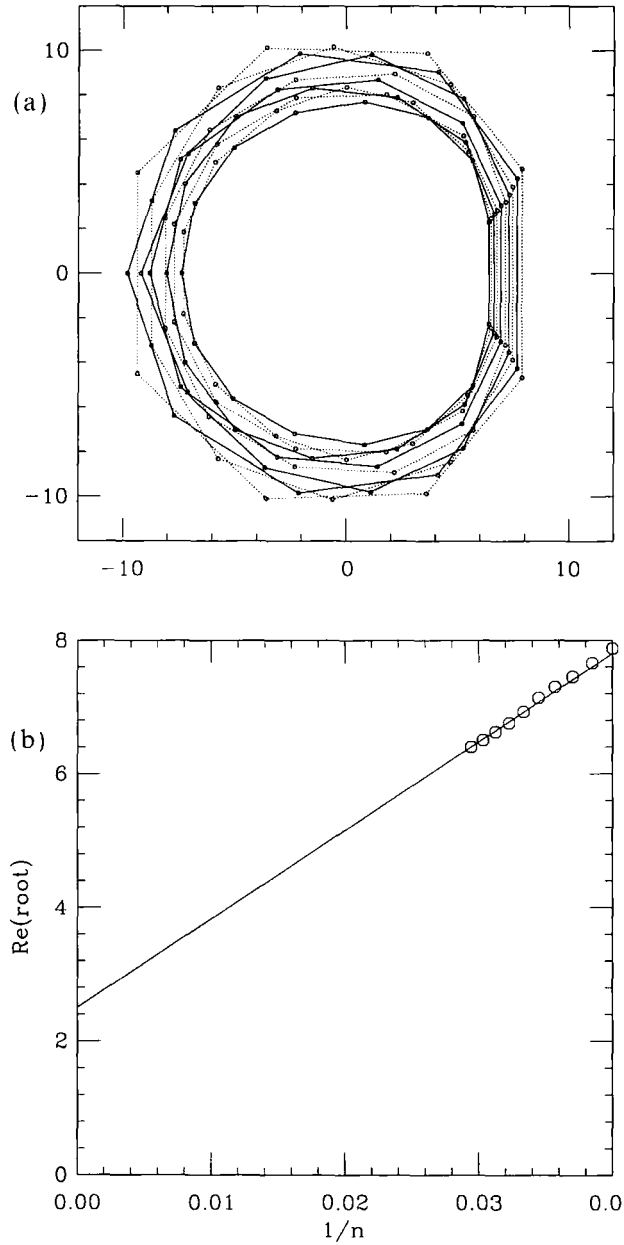

Fig. 4. Left: Zeroes of the polynomial of the partition function for $n = 25 \cdots 34$. Right: The zeroes of the nth root approach the real axis nearly along a straight line, crossing the real axis at $x_c \approx 2.5$.

The coefficients $C_n(m)$ are real and nonnegative, hence none of the roots lies on the real positive axis, but for $n \to \infty$ they will cross it at some point $x_c \leqslant \mu$, since we rigorously know the existence of a phase transition.

We calculated the zeroes of the partition function corresponding to the exact data up to $n = 34$ and plot them in Fig. 4a. The roots seem to lie in nearly perfect circles for every n, but the radius decreases with increasing n. The nth roots nearest to the real positive axis approach the real axis along a nearly straight line. In Fig. 4b we plot the real part of the root nearest to the real axis for $n = 25 \cdots 34$, against $1/n$. Again, the figures are consistent with a transition at $x_c \approx 2.5$.

3. NUMBER OF PARALLEL CONTACTS FOR $\beta = 0$

The second major topic of this paper is to investigate the behavior of the number of parallel contacts m_p in the limit $n \to \infty$. In Fig. 5 we plot

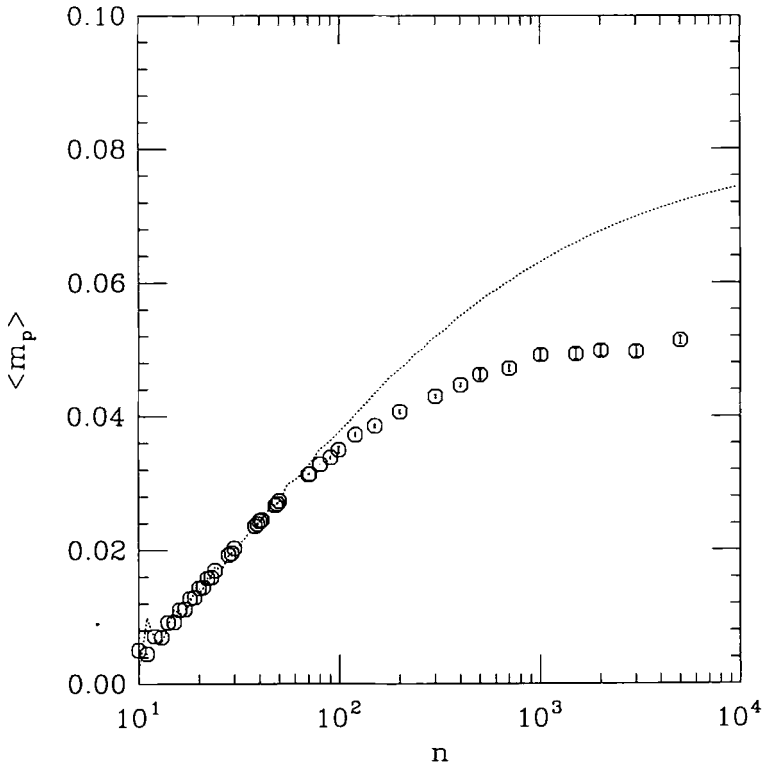

Fig. 5. Expected number of parallel contact as a function of length. The polygons with error bars are Monte Carlo measurements, the dotted line results from Eq. (4) and is an upper bound.

the behavior of $\langle m_p \rangle$ as a function of n, obtained from Eq. (5), which we proposed to be an upper bound. The upper bound reaches asymptotically the value $m_p = 0.08$. Clearly, the earlier mentioned fact that the curve has a somewhat steeper slope at large n and small m_p has impact on $\langle m_p \rangle$, as these configurations are dominant at $\beta = 0$. Therefore we do not use Eq. (5) in the remainder of this section. With Monte Carlo simulations we have determined the expected number of parallel contacts $\langle m_p \rangle$ as a function of n. The results are given in Table III and Fig. 5 and are in agreement with results published by Flesia,[3] but extend to larger values of n. The Monte Carlo results seem to converge to a value around 0.05.

To understand the underlying physics in the regime $\beta = 0$ better, we take a closer look at *where* the parallel contacts are made, and relate this to other types of SAWs. Consider an oriented OSAW of length n, with a parallel contact between the steps i and j of the walk. The sequence of steps from i to j constitutes a polygon of length $l = j - i + 1$, if one of the two steps that form a contact is rotated 90° to close the polygon. The

Table III. Monte Carlo Data for $\langle m_p \rangle$, the Expected Number of Total Parallel Contacts

n	$\langle m_p \rangle$	n	$\langle m_p \rangle$
9	0.001966(3)	10	0.00505(3)
11	0.00450(5)	12	0.00715(3)
13	0.00698(2)	14	0.00918(3)
15	0.00921(3)	16	0.01106(4)
17	0.01118(3)	18	0.01274(4)
19	0.01293(2)	20	0.01429(3)
21	0.01446(4)	22	0.01577(4)
23	0.01592(2)	24	0.01693(7)
28	0.01925(2)	29	0.01953(7)
30	0.02025(3)	38	0.02358(5)
39	0.02389(7)	40	0.02431(8)
41	0.02448(4)	48	0.02667(5)
49	0.02690(8)	50	0.02731(7)
70	0.03129(7)	71	0.03141(5)
80	0.03281(7)	90	0.0338(4)
99	0.0350(5)	120	0.0372(4)
150	0.0385(4)	200	0.0406(4)
300	0.0429(4)	400	0.0446(4)
500	0.0462(7)	700	0.0471(6)
1000	0.0492(9)	1500	0.0493(8)
2000	0.0497(8)	3000	0.0497(9)
5000	0.0514(3)		

remaining sequences of steps from 0 to i and from j to n are two self-avoiding walks of length i and $n-j$, respectively. These two SAWs can be combined into one self-avoiding two-legged star: a SAW of length $n-1$, on which one special point (the origin of the two-legged star) is marked. Note that since the two SAWs are separated by the loop, one being located on the inside of the loop and one on the outside, the two-legged star is always self-avoiding. The mapping of an OSAW with one parallel contact into a rooted polygon plus a two-legged star is illustrated in Fig. 6.

If an OSAW has more than one parallel contact then we can map this OSAW onto different combinations of a rooted polygon plus a two-legged star. In general, if the OSAW has m_p parallel contacts, there are m_p such mappings into a rooted polygon plus a two-legged star. The reverse mapping, i.e., the combination of a two-legged star plus a rooted polygon into an OSAW with a parallel contact, is not guaranteed to result in an OSAW with a parallel contact, as they might cross. Therefore, the total number of rooted polygons of length l times the total number of two-legged stars

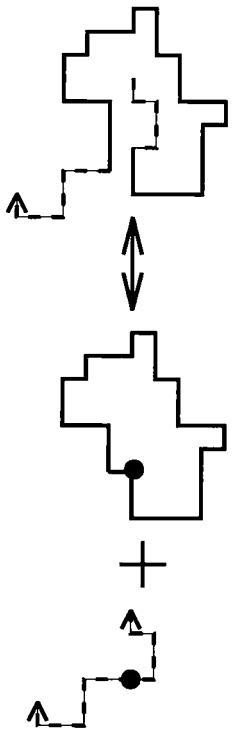

Fig. 6. Decomposition of an OSAW into a loop and a two-legged star.

of length $n-l$, summed over all l, is an upper bound to the number of OSAWs of length n, multiplied by the expectation value of the number of parallel contacts for these walks.

Let us define $f(n, l)$ as the probability that a two-legged star of length $n-l$, if combined with a rooted polygon of length l, results in an OSAW. Then we can write

$$\langle m_p \rangle Z_n = \sum_{m_p} m_p C_n(m_p) = \sum_l P_l S_{n-l} f(n, l) \tag{12}$$

where Z_n, P_n and S_n are the number of OSAWs, rooted polygons and two-legged stars of length n, respectively.

We know that, for large n,

$$Z_n \approx \mu^n n^{\gamma_s - 1} \tag{13}$$

$$S_n \approx \mu^n n^{\gamma_s} \tag{14}$$

$$P_n \approx \mu^n n^{\alpha - 2} \tag{15}$$

Combining this with (12) leads to

$$\langle m_p \rangle = \sum_l \frac{l^{\alpha-2}(n-l)^{\gamma_s} f(n, l)}{n^{\gamma_s - 1}} \tag{16}$$

We can obtain insight in the behavior of the function $f(n, l)$ by means of Monte Carlo simulations. OSAWs are sampled randomly, and for each parallel contact the loop length $l = |j - i + 1|$ is determined, where i and j are the steps making the parallel contact. This procedure gives us $\langle m_p \rangle(l)$, the expectation value of the number of parallel contacts with loop length l. Results for OSAWs with a length $n = 500$, 1000, 2000, and 5000 are plotted in Fig. 7. The quantity $\langle m_p \rangle(l)$ shows a power-law behavior, where the length n of the OSAW is an upper bound to the length l of the loop. It is important, however, that, besides this obvious dependence, the total length n does not appear to have any influence on the behavior of $\langle m_p \rangle(l)$, and this quantity is well described by a power law:

$$\langle m_p \rangle(l) \approx k l^{-\alpha_l} \tag{17}$$

Numerically, we find

$$k = 0.35 \pm 0.1 \tag{18}$$

$$\alpha_l = 1.65 \pm 0.05 \tag{19}$$

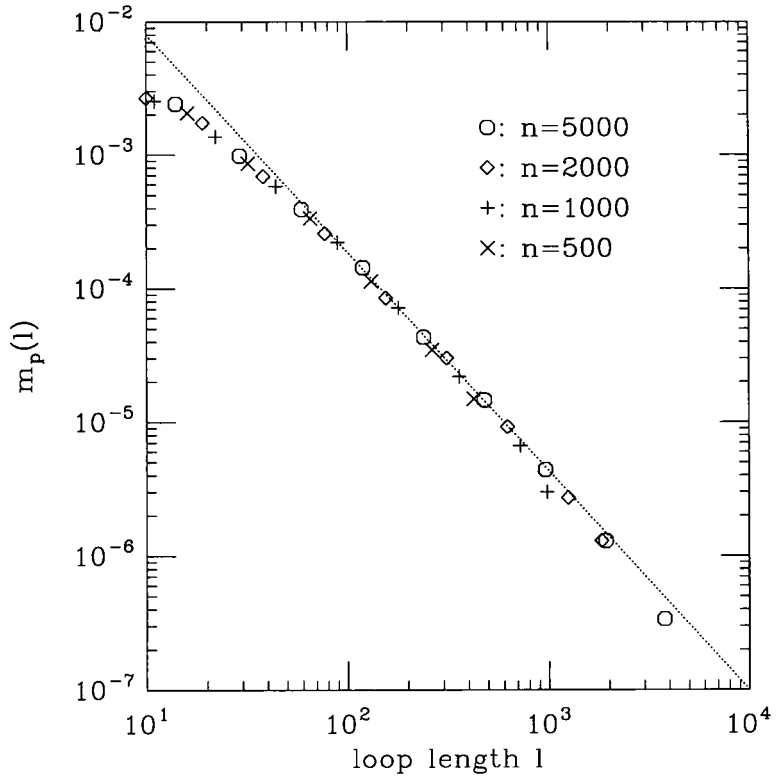

Fig. 7. Probability that an OSAW has a parallel contact with a loop of length l, for OSAWs with a total length $n = 500$, 1000, 2000, and 5000. For each parallel contact, the loop length l is defined as $l = |j - i + 1|$, where i and j are the steps of the OSAW making a parallel contact.

To obtain the mean number of parallel contacts $\langle m_p \rangle$, we sum over all possible (even) lengths l of the rooted polygon:

$$\langle m_p \rangle = \sum_l \langle m_p \rangle(l) \approx k \sum_{l=8}^{n} l^{-\alpha_l} \tag{20}$$

For $n \to \infty$ the right-hand side equals a constant times the function $\zeta(\alpha_l)$, which converges to a constant for $\alpha_l > 1$. This implies again that $\langle m_p \rangle$ tends to a constant, in agreement with earlier Monte Carlo results of Flesia.[3]

The fact that $\langle m_p \rangle$ is constant implies that the SAW critical exponent γ is constant in the free and repulsive regime (i.e., for $\beta \leqslant 0$), and

presumably until the transition. For the exponent γ to change with β, the exponent α_l should be $\leqslant 1$, since this will cause the ζ function to diverge, but this is not supported by our numerical results in Fig. 7.

It is possible to put an upper limit to how far $\langle m_p \rangle$ will still increase if n is increased above 5000: Fig. 7 shows that the contribution of loops with a length below 1000 certainly has converged for $n = 5000$; thus

$$\langle m_p \rangle(\infty) - \langle m_p \rangle(5000) < k \sum_{l=1000}^{n} l^{-\alpha_l} < 10^{-5}$$

A different approach which estimates the number of both parallel and antiparallel contacts is to use the similarity between an OSAW and a twin-tailed tadpole. Consider an OSAW with a contact between steps i and j of the walk. If we add a new edge between steps i and j we obtain an object which we will call a *twin-tailed loop* (see Fig. 8). A twin-tailed loop differs from a nonuniform twin-tailed tadpole only by one edge, and has the same asymptotic behavior. If the contact is parallel, then the twin-tailed loop has one tail inside the loop and the other outside (see Fig. 8a), while if the

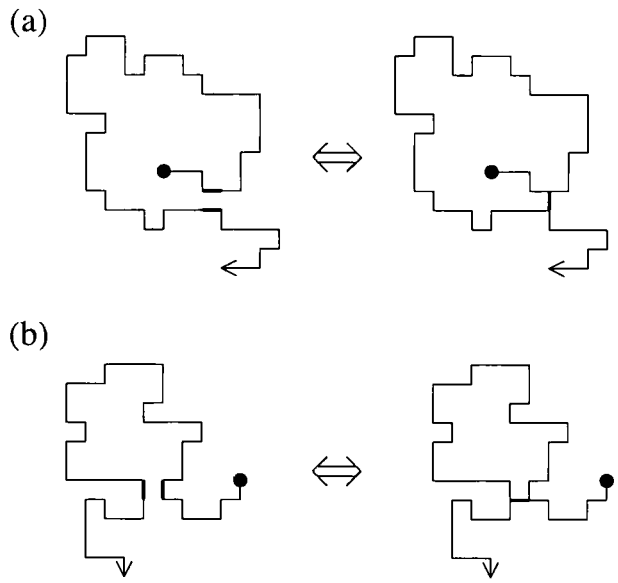

Fig. 8. An OSAW with a contact can be transformed into a twin-tailed loop by adding one step. (a) If the contact was parallel, the twin-tailed loop has one tail on the inside and one on the outside of the loop. (b) If the contact was antiparallel, both tails are located on the outside of the loop.

contact is antiparallel both tails are outside (see Fig. 8b). This is of course only true in two dimensions. Each OSAW with m contacts can be mapped into m distinct twin-tailed loops. If T_n is the total number of twin-tailed loops of total length n, then it follows that

$$T_n = \sum m C_n(m) \tag{21}$$

Dividing both sides by Z_n, where Z_n is the partition function of SAWs, it follows that

$$\langle m \rangle = T_n / Z_n \tag{22}$$

Asymptotically, $Z_n \sim \mu^n n^{\gamma_s - 1}$, where γ_s is the exponent for SAWs. Zhao and Lookman[10] proved that twin-tailed tadpoles have the same growth constant μ as SAWs and that the exponent γ is $\gamma = \gamma_s + 1$. The same kind of proof holds for twin-tailed loops. Replacing these results in Eq. (22) implies the known result $\langle m \rangle \sim n$.

Consider now the parallel and the antiparallel case separately. Twin-tailed loops with both tails outside the loop are the dominant configurations, so they have the exponent γ of the total set, i.e., $\gamma = \gamma_s + 1$. This implies as previously that $\langle m_a \rangle \sim n$ as was proven by Flesia.[3]

Parallel contacts correspond to the subset T_n^* of twin-tailed loops with one tail on the inside and one on the outside of the loop. The question is, what is the value of the exponent γ (let us call this exponent γ_t) for this subset T_n^*? Simple tadpoles (i.e., tadpoles with only one tail) have the same γ as SAWs.[10] Since one element of T_n^* can be constructed from a simple tadpole by adding one edge inside the loop, it follows that $\gamma_t \geqslant \gamma_s$. On the other hand, since T_n^* is a subset of the set of twin-tailed loops, it follows that $\gamma_t \leqslant \gamma_s + 1$, and this inequality can be made strict by considering that $\langle m_p \rangle \sim o(n)$.[2]

We can gain insight into this matter by randomly generating OSAWs of length n, and for each parallel contact determining the length t of the inside tail. Note that if a parallel contact is formed between steps i and j of the OSAW, the steps from i to j form a loop, and "inside" and "outside" tails refer to inside or outside this loop. The results are plotted in Fig. 9. Extrapolating these results, we estimate that the fraction of twin-tailed loops with length t of the inside tail is decreasing as

$$\langle m_p \rangle(t) \sim k_t t^{-\alpha_t} \tag{23}$$

where $\alpha_t = 1.6 \pm 0.1$. The parameters α_t and α_t are within the statistical errors of one another and are probably the same. As in Eq. (23) the parameter α_t exceeds 1, $\sum_t (m_p(t))$ will not be more than a constant times

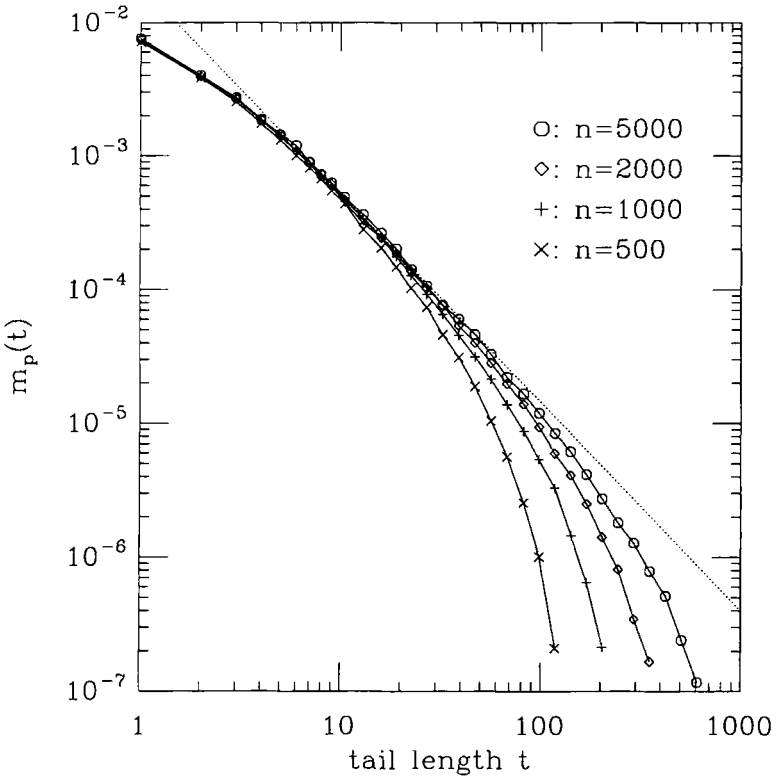

Fig. 9. Probability that an OSAW has a parallel contact with an inside tail of length t for OSAWs with a total length $n = 500$, 1000, 2000, and 5000. For each parallel contact, the steps i up to j form a loop, where i and j are the steps of the OSAW making a parallel contact. The inside tail is defined as those steps of the OSAW that are located within this loop.

$m_p(t=0)$. This implies that T_n^* asymptotically seems to behave as simple tadpoles which have the same γ as SAWs. If we assume, based on these numerical results and intuitive arguments, that the twin-tailed loops with one tail inside and one outside behave as simple tadpoles, then $\gamma_t = \gamma_s$, which would imply that $\langle m_p \rangle$ approaches a constant.

ACKNOWLEDGMENTS

We thank Alan Sokal, John Cardy, John Wheater, and Stu Whittington for fruitful discussions. G.T.B. acknowledges financial support

from the EPSRC under grant GR/J78044, from the DOE under grant DE-FG02-9OER40542, and from the Monell Foundation. S.F. is grateful to EPSRC (United Kingdom) for financial support (grant B/93/RF/1833).

REFERENCES

1. J. L. Cardy, *Nucl. Phys. B* **419**:411 (1994).
2. D. Bennett-Wood, J. L. Cardy, S. Flesia, A. J. Guttmann, and A. L. Owczarek, *J. Phys. A* **28**:5143 (1995).
3. S. Flesia, *Europhys. Lett.* **32**:149–154 (1995).
4. W. M. Koo, *J. Stat. Phys.* **81**:561 (1995).
5. N. Madras and A. Sokal, *J. Stat. Phys.* **56**:109 (1988).
6. B. Nienhuis, *Phys. Rev. Lett.* **49**:1062 (1982).
7. A. Conway, I. G. Enting, and A. J. Guttmann, *J. Phys. A* **26**:1519 (1993).
8. C. N. Yang and T. D. Lee, *Phys. Rev.* **87**:404 (1952).
9. T. D. Lee and C. N. Yang, *Phys. Rev.* **87**:410 (1952).
10. D. Zhao and T. Lookman, *J. Phys. A* **26**:1067–1076 (1993).